Nuclear breakup of ^{8}B in a direct fragmentation model *

R. Shyam[a†] **and H. Lenske**[b]

[a] *Saha Institute of Nuclear Physics, Calcutta - 700 064, India*

[b] *Institut für Theoretische Physik, Universität Giessen, D-35392 Giessen, Germany*

arXiv:nucl-th/9802008v1 3 Feb 1998

Abstract

We calculate the cross sections of the elastic and inelastic breakup modes for the inclusive breakup reaction ^{28}Si(^{8}B,^{7}Be) at beam energies between 10 - 40 MeV/nucleon within a direct fragmentation model formulated in the framework of the post form distorted-wave Born-approximation. In contrast to the case of the stable isotopes, the inelastic breakup mode is found to contribute only up to 30% to the total breakup cross section, which is in agreement with the recently measured experimental data. However, the high energy tail of the energy spectra of ^{7}Be fragment is dominated by the inelastic breakup mode. The breakup amplitude is found to be dominated by contributions from distances well beyond the nuclear surface.

KEYWORDS: Nuclear Breakup of ^{8}B on ^{28}Si, elastic and inelastic breakup cross sections, proton halo in ^{8}B.

PACS NO. 25.60.Gc, 24.10.-i, 25.70.Mn

*Work supported by GSI Darmstadt and BMFT.

†E-mail address: shyam@tnp.saha.ernet.in, associate of Abdus Salam International Centre for Theoretical Physics, Trieste.

1 Introduction

Recently, there has been a lot of interest in the study of the proton drip-line nucleus ^{8}B which is perhaps the most likely candidate for having a proton halo structure [1, 2, 3], since its last proton has a binding energy of only 137 keV. Several measurements reported lately do seem to provide evidence in favor of this possibility. For example, the electric quadrupole moment of ^{8}B is found to be twice as large as the value predicted by the shell model, which can be explained with a single particle wave function corresponding to a matter density of root mean square (rms) radius of 2.72 fm [4]. The observed narrow longitudinal momentum ($p_{\|}$) distribution of the ^{7}Be fragment emitted in the breakup reaction of 1.47 GeV/nucleon ^{8}B on ^{12}C target has been interpreted in terms of a greatly extended proton distribution in ^{8}B [5]. The significantly enhanced reaction cross sections of ^{8}B measured at beam energies between 20 - 60 MeV/nucleon are shown to be consistent with the large matter radius of ^{8}B required to explain its quadrupole moment [6].

Nevertheless, the existence of a proton halo in ^{8}B is still an open issue. Nakada and Otsuka [7] have shown that $(0+2)\hbar\omega$ shell model calculations can reproduce the measured large quadrupole moment of ^{8}B without invoking a proton halo structure. The interaction cross sections measured by Tanihata et al. [8] at 790 MeV/nucleon are consistent with a normal size of ^{8}B. The $p_{\|}$ distribution of the ^{7}Be fragment emitted in the breakup reaction of ^{8}B at 41 MeV/nucleon has been found to be dependent on the target mass in Ref. [9] where it is argued that in contrast to the situation in the neutron halo nuclei [10, 11], the assumption of an unusually extended spatial distribution is not necessary to explain the narrow $p_{\|}$ distribution in case of ^{8}B; the reaction mechanism plays an important role here.

Breakup reactions in which the halo particle(s) is(are) removed from the projectile in the Coulomb and nuclear fields of the target nucleus, have played a

significant role in probing the neutron halo structure in some light neutron drip-line nuclei (see e.g. [12] for a recent review). The enhanced total Coulomb breakup cross sections [13, 14], narrow longitudinal momentum distributions of the heavy fragments [10, 15, 16], and sharply forward peaked angular distributions of the valence neutron(s) [17, 18] are some of the pivotal observations through which the neutron halo structure has been well manifested.

Apart from the $p_{\|}$ distributions of the ^{7}Be fragment, some data on the total cross section of the breakup reaction $^8\mathrm{B} + \mathrm{A} \rightarrow {}^7\mathrm{Be} + \mathrm{X}$ on low mass targets have also become available recently [19]. The theoretical studies reported so far have used either the Serber type [20] of models [19, 21] or the diffraction dissociation picture [22] developed by Sitenko and co-workers [23]. Both these approaches are essentially semi-classical in nature, hence a more microscopic calculation within the quantum mechanical scattering theory is needed to interpret the data properly. A proper understanding of the nuclear breakup of ^{8}B is also important in the context of the extraction of the astrophysical S-factor for the radiative capture reaction $^7\mathrm{Be}(\mathrm{p},\gamma)^8\mathrm{B}$ from the Coulomb dissociation of ^{8}B [24, 25].

In this paper, we present calculations of the cross sections for the breakup reaction $^8\mathrm{B} + {}^{28}\mathrm{Si} \rightarrow {}^7\mathrm{Be} + \mathrm{X}$ within a direct fragmentation model (DFM), which is formulated in the framework of the post form distorted wave Born approximation (PFDWBA) [26, 27, 28]. As the target nucleus involved in this reaction is very light, we shall consider only the nuclear breakup process. However, the Coulomb breakup can also be calculated in this theory on the same footing (see e.g. [26]). In the next section we present the details of our formalism. In section 3, our results are presented and discussed. The conclusions of our work are described in section 4.

2 Formalism

The nuclear breakup cross section consists of two components: the elastic breakup (ELB) (also known as "diffraction dissociation") where X corresponds to the target nucleus A in its ground state and proton, and inelastic breakup (INELB) (also known as "diffraction stripping") where X can be any other channel of the A + p system. The triple differential cross section for the elastic breakup reaction $a + A \rightarrow c + x + A$ (e.g for our case, $a = {}^8$B, $c = {}^7$Be, $x =$ p), is defined as

$$\frac{d^3\sigma^{ELB}(a,c)}{d\Omega_c dE_c d\Omega_x} = 2\pi \frac{\mu_a \mu_c \mu_x}{(2\pi\hbar)^6} \frac{q_c q_x}{q_a} \sum_{\ell m_\ell} \mid \beta^{ELB}_{\ell m_\ell} \mid^2, \quad (1)$$

where the transition amplitude $\beta_{\ell m_\ell}$ is given by

$$\sqrt{(2\ell+1)}\beta^{ELB}_{\ell m_\ell} = \int dr_{cx} dR_i \chi^{(-)*}(\mathbf{q}_c, \mathbf{R}_f) \chi^{(-)*}(\mathbf{q}_x, \mathbf{R}_x) \times V_{cx}(\mathbf{r}_{cx}) u_\ell(r_{cx}) y_{\ell m_\ell}(\hat{r}_{cx}) \chi^{(+)}(\mathbf{q}_a, \mathbf{R}_i). \quad (2)$$

In Eqs. (1) and (2), ℓ is the orbital angular momentum for relative $c + x$ system and $y_{\ell m_\ell}$ are the spherical harmonics. V_{cx} represents the interaction between constituents c and x while u_ℓ is the wave function for their relative motion in the projectile ground state. $\mathbf{q}_a$ (μ_a), $\mathbf{q}_c$ (μ_c) and $\mathbf{q}_x$ (μ_x) are the momenta (reduced masses) of the particles a, c and x respectively. χ's denote the scattering wave functions which are generated by the appropriate optical potentials in respective channels. The system of coordinates used are the same as that given in Ref. [27].

The transition amplitude is a six dimensional integral. By making a zero range approximation (ZRA) this integral is reduced to three dimensions [29], although its calculation is still a major problem as it involves a product of three scattering waves which converge very slowly. In the ZRA the details of the internal structure of the projectile appear in the amplitude only through an overall normalization constant and the values of ℓ other than zero are necessarily excluded. Because of the relative p-state between ^{7}Be and the proton in the ground state

of ^{8}B the ZRA, therefore, is not suitable for this case. However, we introduce a constant range approximation (CRA) which reduces the integral in Eq. (2) to three dimensions and at the same time allows the non-zero values of ℓ to enter in the calculations. We assume that the breakup reaction is strongly peripheral and that only those configurations where (1) the proton is in the collinear position between the target nucleus and ^{7}Be and (2) the relative separation between proton and ^{7}Be is constant (say $d\ fm$), contribute to the transition amplitude. We can then write

$$V(\mathbf{r}_{cx})u_\ell(r_{cx})y_{\ell m_\ell}(\hat{r}_{cx}) \;=\; D_a\delta(\mathbf{r}_{cx}-d\frac{\mathbf{R}_i}{R_i})y_{\ell m_\ell}(\hat{R}_i), \tag{3}$$

where d is taken to be the distance between origin and the maximum in the ^{8}B ground state wave function. Approximations similar to the CRA have been used earlier by Pühlhoffer et al. [30] and Kubo and Hirata [31] to study the α transfer reactions induced by ^{6}Li and ^{7}Li projectiles within the DWBA. These authors have found a reasonable agreement between the calculated and measured angular distributions particularly for momentum matched transitions. Furthermore, as long as the reaction is not sensitive to the smaller distances, the results obtained with Eq. (3) are in agreement with those of the full finite range calculations.

Substituting Eq. (3) in Eq. (2), making partial wave expansion for $\chi^{(-)*}(\mathbf{q}_x,\mathbf{R}_x)$ and using Eq. (4.13) of [32], we get

$$\begin{aligned}\beta^{ELB}_{\ell m_\ell} &= \sqrt{4\pi}D_a\sum_{\ell_x m_x}\sum_{LM_L}\imath^{-\ell_x}(-)^{m_x}\sqrt{\frac{2\ell_x+1}{2L+1}}y_{\ell_x m_x}(\hat{q}_x)\\ &\quad\times <\ell_x -m_x\ell m_\ell \mid LM_L><\ell_x 0\ell 0\mid L0>\tilde{\beta}^{ELB}_{\ell m_\ell},\end{aligned} \tag{4}$$

where the reduced amplitude $\tilde{\beta}^{ELB}_{\ell m_\ell}$ is given by

$$\tilde{\beta}^{ELB}_{\ell m_\ell} \;=\; \int dR_i\chi^{(-)*}(\mathbf{q}_c,\alpha_1\mathbf{R}_i)\frac{\chi_{\ell_x}(q_x,\alpha_2R_i)}{\alpha_2 q_x R_i}y_{LM_L}(\hat{R}_i)\chi^{(+)}(\mathbf{q}_a,\mathbf{R}_i). \tag{5}$$

In Eq. (5) we have

$$\alpha_1 \;=\; \frac{m_A}{m_A+m_x}+(1-\frac{m_A}{m_A+m_x}\frac{m_c}{m_a})\frac{d}{R_i}, \tag{6}$$

$$\alpha_2 = 1 - \frac{m_c}{m_a}\frac{d}{R_i}, \quad (7)$$

and χ_{ℓ_x} is the radial part of the wave function $\chi^{(-)*}(\mathbf{q}_x, \mathbf{R}_x)$. Eq. (5) is similar to the amplitude obtained with the ZRA and can be evaluated by using the method described in e.g. [28]. The expressions for the zero range amplitudes are retrieved from Eq. (4) - Eq. (6) by assuming ℓ and d equal to zero.

The transition amplitude for the inelastic breakup reaction $a + A \rightarrow c + C$, where C is some final state of the system $A + x$, is given by [27]

$$\sqrt{(2\ell+1)}\beta^{INELB}_{\ell m_\ell} = \int dr_{cx} dR_i \chi^{(-)*}(\mathbf{q}_c, \mathbf{R}_f)\chi^C(\mathbf{q}_x, \mathbf{R}_x) \times V_{cx}(\mathbf{r}_{cx}) u_\ell(r_{cx}) y_{\ell m_\ell}(\hat{r}_{cx})\chi^{(+)}(\mathbf{q}_a, \mathbf{R}_i), \quad (8)$$

where $\chi^C(\mathbf{q}_x, \mathbf{R}_x)$ is the form factor, which is obtained by taking the overlap of the wave function for the channel C (which incorporates all the possible reactions initiated by the interaction between nuclei A and x), with the wave function describing the internal states of the target and projectile nuclei. Using Eq. (3) and other steps as described above, an expression similar to Eq. (4) can be derived for $\beta^{INELB}_{\ell m_\ell}$ with the reduced amplitude given by

$$\tilde{\beta}^{INELB}_{\ell m_\ell} = \int dR_i \chi^{(-)*}(\mathbf{q}_c, \alpha_1 \mathbf{R}_i)\frac{\chi^C_{\ell_x}(q_x, \alpha_2 R_i)}{\alpha_2 q_x R_i} y_{LM_L}(\hat{R}_i)\chi^{(+)}(\mathbf{q}_a, \mathbf{R}_i), \quad (9)$$

where $\chi^C_{\ell_x}$ is the radial part of the form factor. Its calculation simplifies greatly if we introduce the so called "surface approximation" and write $\chi^C_{\ell_x}$ in terms of its asymptotic form

$$\chi^C_{\ell_x}(q_x, R_i) = \frac{1}{2} S_{\ell_x, C} H^{(+)}_{\ell_x}(q_x, R_i), \quad (10)$$

where $H^{(+)}_{\ell_x} = G_{\ell_x} + \imath F_{\ell_x}$, with F_{ℓ_x} and G_{ℓ_x} being the regular and irregular Coulomb wave functions. This equation can be rewritten in terms of the elastic scattering wave function χ_{ℓ_x} (see Eq. (5)) as

$$\chi^C_{\ell_x}(q_x, R_i) = \frac{S_{\ell_x, C}}{S_{\ell_x, \ell_x} - 1}(\chi_{\ell_x}(q_x, R_i) - F_{\ell_x}(q_x R_i)), \quad (11)$$

where S_{ℓ_x,ℓ_x} are the S matrix elements for the elastic channel corresponding to the angular momentum ℓ_x. The validity of the surface approximation has been tested by Kasano and Ichimura [33] who found it to be well fulfilled even for the deuteron. We use Eq. (11) for the form factor $\chi^C_{\ell_x}$ also in the interior region in Eq. (9), which is not expected to be a serious approximation as this region contributes very little to the whole DWBA integral. In order to calculate the inelastic breakup cross section one has to sum over all the channels $C \neq \ell_x$, which can be easily done by using the unitarity of the S matrix as all the dependence on channel C in the transition amplitude rests in the S matrix $S_{\ell_x,C}$

$$\sum_{C\neq\ell_x} \mid S_{\ell_x,C} \mid^2 \;=\; 1- \mid S_{\ell_x,\ell_x} \mid^2 \tag{12}$$

Thus the inelastic breakup cross section can be written as

$$\frac{d^3\sigma^{INELB}(a,c)}{d\Omega_c dE_c d\Omega_x} \;=\; 2\pi\frac{\mu_a\mu_c\mu_x}{(2\pi\hbar)^6}\frac{q_c q_x}{q_a}\sum_{\ell m_\ell}(\sigma^{REAC}_{\ell_x}/\sigma^{ELAS}_{\ell_x}) \mid \beta^{ELB}_{\ell m_\ell} - \beta^0_{\ell m_\ell} \mid^2, \tag{13}$$

where $\beta^0_{\ell m_\ell}$ is the same as the amplitude defined in Eq. (4) with the wave function χ_{ℓ_x} replaced by the regular Coulomb function. The partial reaction and elastic cross sections $\sigma^{REAC}_{\ell_x}$ and $\sigma^{ELAS}_{\ell_x}$ are related to the scattering matrix elements S_{ℓ_x,ℓ_x} by their usual definitions. It may be noted that the quantities required to calculate the inelastic breakup are the same as those already calculated in the case of elastic breakup.

In order to study the impact parameter dependence of the breakup cross section, we define the "probability of breakup" $T^{b-up(a,c)}_{\ell_a}$ as

$$\sigma^{b-up(a,c)}_{total} \;=\; \int dE_c d\Omega_c d\Omega_x \frac{d^3\sigma(a,c)}{dE_c d\Omega_c d\Omega_x} \tag{14}$$

$$\;=\; (\pi/q_a^2)\sum_{\ell_a}(2\ell_a+1)T^{b-up(a,c)}_{\ell_a} \tag{15}$$

In Eq. (14), $d^3\sigma(a,c)/dE_c d\Omega_c d\Omega_x$ is the sum of the elastic and inelastic breakup cross sections given by Eqs. (1) and (13).

3 Results and discussion

The optical potentials in the entrance and outgoing channels and the constants D_a and d are required as input in our numerical calculations. Although some elastic scattering data for the ^{8}B, ^{7}Be + ^{12}C systems at the beam energy of 40 MeV/nucleon are available [34], the usual optical model fits to them is unfortunately not reported. Unless otherwise stated, our calculations have been performed with the following set of optical potentials, V_R = 123.0 MeV, r_V = 0.75 fm, a_V = 0.80 fm, W = 65.0 MeV, r_W = 0.78 fm, a_W = 0.80 fm, with real and imaginary volume Woods-Saxon terms. This potential, which is similar to that used in the recent analysis of ^{9}Li and ^{11}Li elastic scattering [35], has been used for both ^{8}B and ^{7}Be. The $(A^{1/3} + a^{1/3})$ convention was followed to get the radii from the radius parameters. The global Becchetti-Greenlees parameterization [36] was used for the proton-target potential.

The constants D_a (see e.g. [31]) and d have been determined with a ^{8}B ground state wave function obtained by assuming it to be a pure $0p_{3/2}$ proton single particle state, with separation energy 0.137 MeV, calculated in a central Woods-Saxon potential of geometry, r_0 = 1.54 fm, and a_0 = 0.52 fm [37]. This gives D_a = -39.0 MeV fm$^{3/2}$ and d = 1.8 fm, which has been used in all the calculations described in this paper. The radius and diffuseness parameters used by Barker [38] (r_0 = 1.25 fm, and a_0 = 0.65 fm), and Esbensen and Bertsch (r_0 = 1.25 fm, and a_0 = 0.52 fm) [39] lead to D_a = -40.4 and -41.7 MeV fm$^{3/2}$ and d = 1.8 and 1.7 fm respectively. On the other hand, with more elaborate RPA models for the ^{7}Be + p overlap wave function [5], the values of D_a and d are found to be -38.0 MeV fm$^{3/2}$ and 1.8 fm respectively. Hence, the constants D_a and d do not show any marked dependence on the nuclear structure model of ^{8}B. For the sake of comparison with other approaches the simplified potential model as used by us seems to be adequate at this stage of the present theory.

Fig. 1 shows the calculated elastic (dotted line), inelastic (dashed line) and total (solid line) breakup cross sections for the ^{8}B + ^{28}Si $\rightarrow$ ^{7}Be + X reaction as a function of beam energy together with the data taken from [19]. We see that the measured total breakup cross sections are well reproduced by our calculations although the contributions of the elastic and inelastic breakup modes are slightly over- and under-predicted respectively. The breakup cross sections decrease with beam energy up to 20 MeV/A and after that they are almost constant (although the inelastic breakup mode still shows a tendency of decreasing somewhat). The nuclear breakup cross sections of ^{8}B as reported in [22, 19] show a similar type of energy dependence in this beam energy regime although their increase below 20 MeV/nucleon is less pronounced than that seen in Fig. 1. Clearly, more measurements are needed to clarify this point.

A striking feature of the results shown in Fig. 1 is that the contribution of the inelastic breakup mode to the total breakup cross section is limited only to about 30%, which is in agreement with the experimental data [19]. This is in marked contrast to the situation in stable nuclei where this mode of breakup makes up about 75 - 80 % of the total (a, c) breakup cross section (see e.g. [28]). To understand this difference, we show in Fig. 2 the breakup probability (T_ℓ) (defined by Eq. (14)) for the reaction ^{28}Si(^{8}B, ^{7}Be) as a function of the impact parameter b ($b = (\ell_d + 1/2)/q_a$). It can be seen that T_ℓ peaks at about 8 fm, which is in remarkable agreement with that obtained in Ref. [19] from the semi-classical arguments. This is quite large in comparison to the sum of the radii (R_s) of ^{8}B and ^{28}Si ($\simeq$ 6 fm). Furthermore, most of the contribution to T_ℓ comes from the impact parameters beyond 8 fm, while those from distances $< R_s$ are strongly suppressed. This clearly shows that the breakup of ^{8}B takes place far away from the nuclear surface which reduces the probability of the inelastic breakup process; large impact parameters favor the elastic breakup mode. In contrast, for stable

isotopes, the breakup probability peaks around R_s (where the inelastic breakup mode is maximum) and the drop from the peak value for $b > R_s$ is much faster than that seen in Fig. 2 [28, 41]. This, explains to some extent the difference in the nature of the inelastic breakup cross section of ^{8}B as compared to that of the stable isotopes. The fact that the breakup of ^{8}B is dominated by contributions coming from a large range of impact parameters $> R_s$, is in agreement with the observation made earlier in the case of neutron halo nuclei ^{11}Li and ^{11}Be [26]. This could provide an indirect evidence for a larger spatial extension of the proton in the ground state of ^{8}B. It should, however, be stressed that a $0p_{3/2}$ configuration for the p - ^{7}Be relative motion already leads to a ^{8}B matter density with a larger rms radius [7, 40]. Nevertheless, in the present calculations the ^{8}B structure input largely affects only the absolute magnitudes of the cross sections (through the constant D_a); the peak position in Fig. 2 is mostly decided by the reaction dynamics. It is possible, in principle, to include other components (eg. $p_{1/2}$, $f_{7/2}$) in the ^{8}B wave function within this formalism. However, as the $0p_{3/2}$ component carries by far the largest spectroscopic weight (> 90 %), this is unlikely to alter our results much.

As a side remark, we point out that the relative contributions of the elastic and inelastic breakup modes are independent of the uncertainties in the values of D_a and d as the same constants enter in all the cross sections.

In Fig. 3, we show the contributions of elastic and inelastic breakup modes to the energy distribution of the ^{7}Be fragment at the beam energy of 30 MeV/nucleon. One notes that while the elastic breakup mode dominates in the peak region, its contribution is very weak towards the high energy end (where the proton energy $E_p \rightarrow 0$); total cross section is made up mostly of the inelastic breakup mode in this region. The threshold behavior of the breakup cross section can be easily understood from that of the phase-shift δ_p of the scattering of the proton from

the target. It can be shown that [41] in the limit $E_p \rightarrow 0$, the elastic and inelastic breakup cross sections are proportional to $q_p^{2\ell_p+1}$ and $R^{2\ell_p+1}$ (where R is the radius of the nuclear potential) respectively. Therefore, in this limit the elastic breakup cross section tends to zero even for the $s-$ wave A + p interaction while the inelastic one to a finite value, which explains the observation made in Fig. 3. It would be very interesting therefore, to perform measurements for the energy spectra of the fragment ^{7}Be to confirm the $E_p \rightarrow 0$ behavior. It may help in fixing the absolute magnitude of the inelastic breakup cross section in the breakup experiments.

4 Conclusions

To conclude, we have presented for the first time a fully quantum mechanical calculation of the elastic and inelastic modes of the nuclear breakup of ^{8}B on the Si target. We employed a direct fragmentation model which is formulated within the framework of the post form distorted wave Born-approximation. This is a definite improvement over the semi-classical models of the breakup reactions used so far for this purpose. We obtain a good overall description of the experimental data measured recently. The inelastic breakup mode is found to contribute only up to 30% to the total breakup cross section for the ^{28}Si(^{8}B,^{7}Be) reaction, which is in contrast to the breakup of the stable isotopes. Most of the contributions to the breakup cross section come from the distances far beyond the nuclear surface which favors the elastic breakup mode.

The energy spectra of the ^{7}Be fragment is dominated by the inelastic breakup mode towards the high energy end where the proton energy goes to zero. This observation which is beyond the scope of the semi-classical models, is a natural outcome of the PFDWBA theory of the breakup reactions and it should be verified experimentally.

We must stress that the lack of the precise knowledge about the parameters of the optical potential for the ^{8}B,^{7}Be + ^{28}Si system is a potential source of uncertainty in our calculations. Therefore, the analysis of the existing data (taken at around 40 MeV/nucleon) for this system [34] in terms of the conventional optical model would be extremely useful. Moreover, similar studies at other beam energies are also clearly needed. The present calculations are not very sensitive to the nuclear structure models of ^{8}B. The direct fragmentation model should be improved further so that more detail of the projectile wave function can enter in the calculations explicitly. Once such an extended reaction description is available, the use of more elaborate nuclear structure models of the projectile will be meaningful. It may then become possible to use the breakup data to distinguish the wave functions of ^{8}B obtained from a static potential model from those calculated from dynamical approaches [5] where the deformation of this nucleus is taken into account.

Useful discussions with Hans Geissel is gratefully acknowledged. Thanks are also due to Ulrich Mosel for his very kind hospitality to one of us (RS) in the University of Giessen.

References

[1] H. Kitagawa and H. Sagawa, Phys. Lett.B **299**, 1 (1993).

[2] K. Riisager and J.S. Jensen, Phys. Lett.B **301**, 6 (1993).

[3] K. Riisager, Rev. Mod. Phys. **66**, 1105 (1994)

[4] T. Minamisono et al., Phys. Rev. Lett. **69**, 2058 (1992).

[5] W. Schwab et al., Z. Phys.A **350**, 283 (1995).

[6] R.E. Warner et al., Phys. Rev.C **52**, R1166 (1995).

[7] H. Nakada and T. Otsuka, Phys. Rev.C **49**, 886 (1994).

[8] I. Tanihata et al., Phys. Lett.B **206**, 592 (1988).

[9] J.H. Kelley et al., Phys. Rev. Lett. **77**, 5020 (1997).

[10] J.H. Kelley et al., Phys. Rev. Lett. **74**, 30 (1995).

[11] P. Banerjee and R. Shyam, J. Phys.G: Nucl. Part. Phys. **22**, L79 (1996).

[12] P.G. Hansen, A.S. Jensen and B. Jonson, Ann. Rev. Nucl. Part. Sci. **45**, 2 (1995).

[13] B. Blank et al., Z. Phys.A **340**, 41 (1991).

[14] D. Sacket et al., Phys. Rev.C **48**, 118 (1993).

[15] T. Kobayashi et al., Phys. Rev. Lett. **60**, 2599 (1988).

[16] N.A. Orr et al., Phys. Rev.C **51**, 3116 (1995).

[17] R. Anne et al., Phys. Lett.B **250**, 19 (1990).

[18] R. Anne et al., Nucl. Phys.A **575**, 125 (1994).

[19] F. Negoita et al., Phys. Rev.C **54**, 1787 (1996).

[20] R. Serber, Phys. Rev. **72**, 1008 (1947).

[21] P.G. Hansen, Phys. Rev. Lett. **77**, 1016 (1996).

[22] K. Hencken, G. Bertsch and H. Esbensen, Phys. Rev.C **54**, 3043 (1996).

[23] A. G. Sitenko, *Theory of Nuclear Reactions* (World Scientific, Singapore, 1990).

[24] S. Typel, H.H. Wolter and G. Baur, Nucl. Phys.A **613**, 147 (1997)

[25] T. Kikuchi et al., Phys. Lett.B **391**, 261 (1997)

[26] R. Shyam, P. Banerjee and G. Baur, Nucl. Phys.A **540**, 341 (1992).

[27] R. Shyam and M.A. Nagarajan, Ann. Phys. **163**, 265 (1985).

[28] G. Baur, F. Rösel, D. Trautmann, and R. Shyam, Phys. Rep. **111**, 333 (1984).

[29] G.R. Satchler, *Direct Nuclear Reactions* (Oxford Uni. Press, New York, 1983).

[30] F. Pühlhofer, H.G. Ritter, R. Bock, G. Brommundt, H. Schmidt, and K. Bethge, Nucl. Phys.A **147**, 258 (1970).

[31] K.I. Kubo and M. Hirata, Nucl. Phys. **187**, 186 (1972).

[32] D.M. Brink and G.R. Satchler, *Angular Momentum* (Clarendon Press, Oxford, 1993).

[33] A. Kasano amd M. Ichimura, Phys. Lett.B **115**, 81 (1982).

[34] I. Pecina et al., Pkys. Rev.C **52**, 191 (1995).

[35] M. Zahar et al., Phys. Rev.C **54**, 1262 (1996).

[36] F.D. Becchetti and G.W. Greenlees, Phys. Rev. **182**, 1190 (1969).

[37] K.H. Kim, M.H. Park and B.T. Kim, Phys. Rev.C **35**, 363 (1987).

[38] F.C. Barker, Aust. J. Phys. **33**, 177 (1980).

[39] H. Esbensen and G.F. Bertsch, Nucl. Phys.A **600**, 37 (1996).

[40] B.A. Brown, A. Csoto and R. Sherr, Nucl. Phys.A **597**, 66 (1996)

[41] G. Baur, R. Shyam, F. Rösel and D. Trautmann, Helv. Phys. Acta, **53**, 506 (1980); G. Baur, Proc. Varna Int. Summer School on Nuclear Pysics, Sept. 22 - Oct. 1, 1985, Varna, Romania (unpublished).

Figure Captions

Fig. 1. Total cross section for the breakup reaction of ^{8}B + ^{28}Si $\rightarrow$ ^{7}Be + X as a function of the beam energy. The contributions of the elastic and inelastic breakup modes are shown by dotted and dashed lines respectively while their sum is depicted by the solid line. The experimental data for the total (solid circles), elastic (solid squares) and inelastic (open circles) breakup cross sections are taken from [19].

Fig. 2. Breakup probability (T_l) (as defined by Eq. (14)) for the reaction studied in Fig. 1 at the beam energy of 40 MeV/nucleon as a function of the impact parameter.

Fig. 3. Energy distribution of the ^{7}Be fragment emitted in the breakup of ^{8}B on ^{28}Si target at the beam energy of 30 MeV/nucleon. The solid, dashed and dotted lines have the same meaning as in Fig. 1.

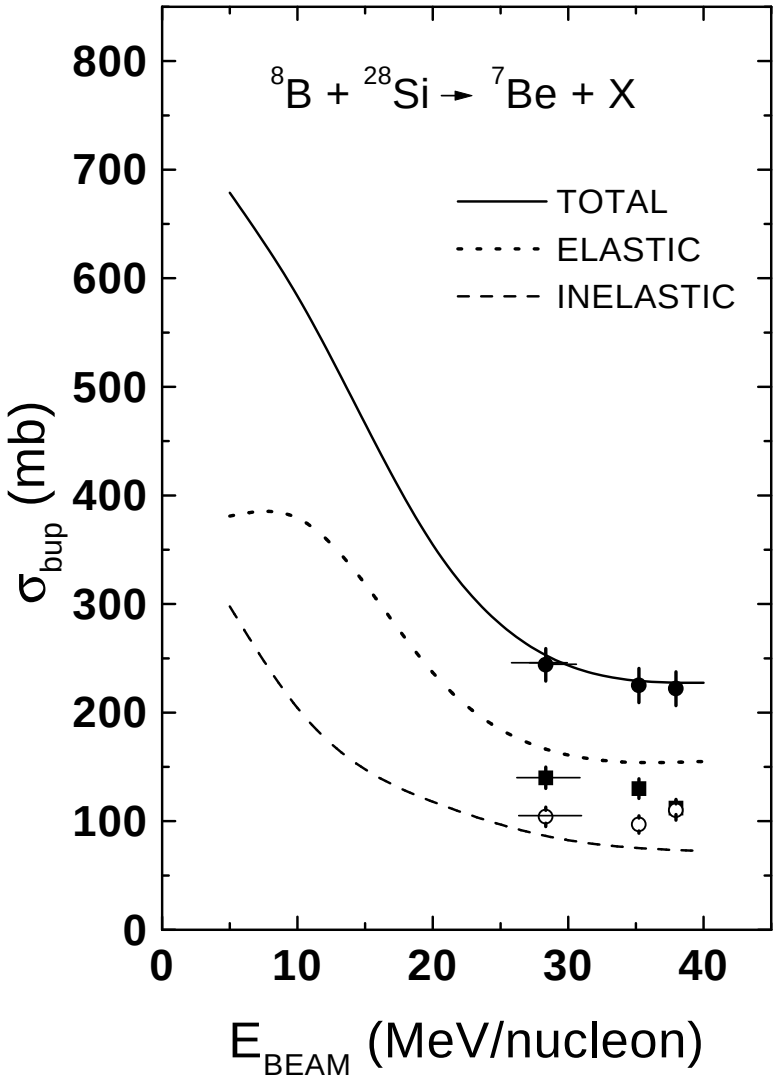

Figure 1: Total cross section for the breakup reaction of ^{8}B + ^{28}Si $\rightarrow$ ^{7}Be + X as a function of the beam energy. The contributions of the elastic and inelastic breakup modes are shown by dotted and dashed lines respectively while their sum is depicted by the solid line. The experimental data for the total (solid circles), elastic (solid squares) and inelastic (open circles) breakup cross sections are taken from [19].

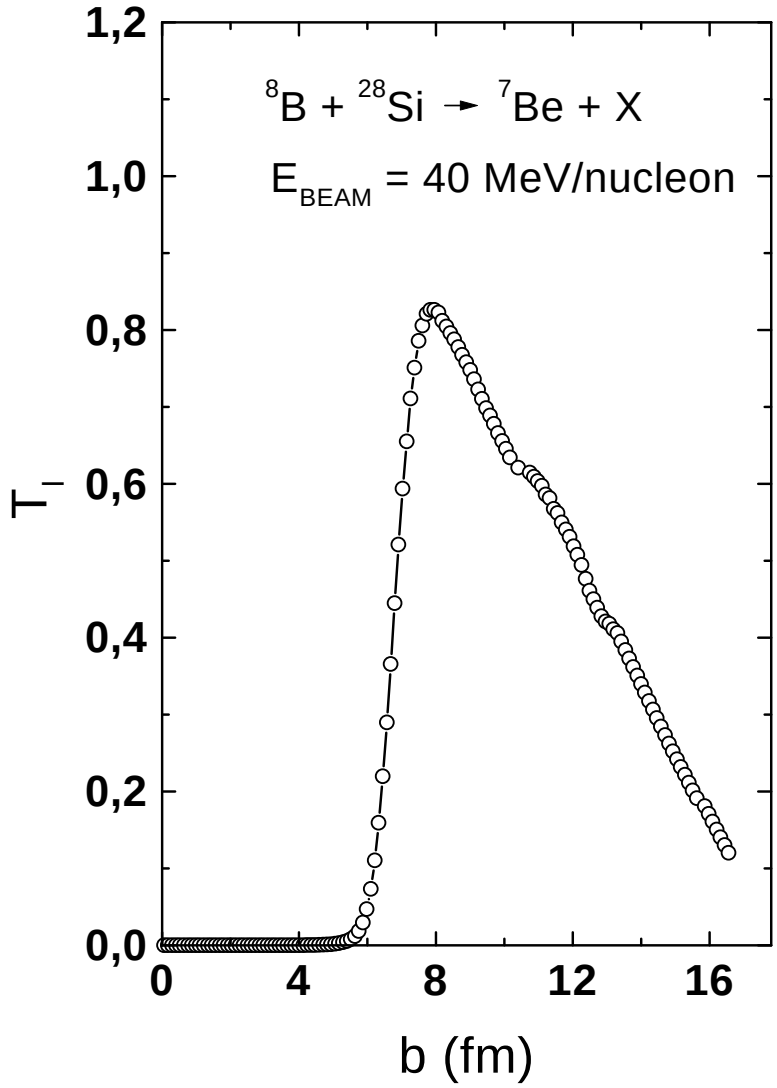

Figure 2: Breakup probability (T_l) (as defined by Eq. (14)) for the reaction studied in Fig. 1 at the beam energy of 40 MeV/nucleon as a function of the impact parameter.

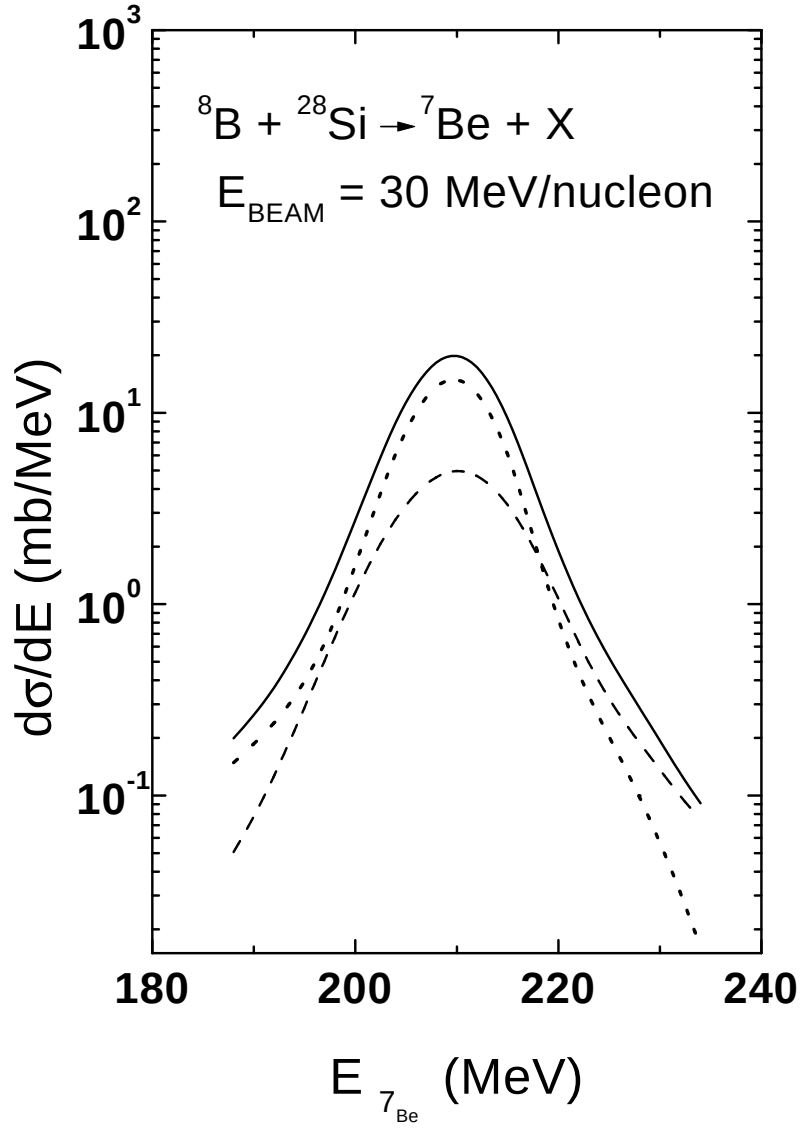

Figure 3: Energy distribution of the ^{7}Be fragment emitted in the breakup of ^{8}B on ^{28}Si target at the beam energy of 30 MeV/nucleon. The solid, dashed and dotted lines have the same meaning as in Fig. 1.